CDF Note 10622-CONF

D0 Note 6231-CONF

Combination of CDF and D0 measurements of the W boson helicity in top quark decays

The CDF and D0 Collaborations

We report the combination of recent measurements of the helicity of the W boson from top quark decay by the CDF and D0 collaborations, based on data samples of 2.7 – 5.4 fb^{-1} of $p\bar{p}$ collisions collected during Run II of the Fermilab Tevatron Collider. Combining measurements that simultaneously determine the fractions of W bosons with longitudinal (f_0) and right-handed (f_+) helicities, we find $f_0 = 0.732 \pm 0.081$ [$\pm$ 0.063 (stat.) $\pm$ 0.052 (syst.)] and $f_+ = -0.039 \pm 0.045$ [$\pm$ 0.034 (stat.) $\pm$ 0.030 (syst.)]. Combining measurements where one of the helicity fractions is fixed to the value expected in the standard model, we find $f_0 = 0.685 \pm 0.057$ [$\pm$ 0.035 (stat.) $\pm$ 0.045 (syst.)] and $f_+ = -0.013 \pm 0.035$ [$\pm$ 0.018 (stat.) $\pm$ 0.030 (syst.)]. The results are consistent with standard model expectations.

Preliminary Results for Summer 2011 Conferences

I. INTRODUCTION

The study of the properties of the top quark t is one of the major topics of Run II of the Tevatron proton-antiproton Collider program at Fermilab. Using data samples two orders of magnitude larger than were available when the top quark was first observed [1, 2], the CDF and D0 collaborations have investigated many properties of the top quark, including the helicity of the W bosons produced in the decays $t \to Wb$. The on-shell W bosons from top quark decays can have three possible helicity states, and we denote the fraction of W bosons produced in these states as f_0 (longitudinal), f_- (left-handed), and f_+ (right-handed). In the standard model (SM), the top quark decays via the $V-A$ weak charged-current interaction, which strongly suppresses right-handed W bosons. The SM expectation for the helicity fractions depends upon the masses of the top quark (m_t) and the W boson (M_W). For the current world average values $m_t = 173.3 \pm 1.1$ GeV/c^2 [3] and $M_W = 80.399 \pm 0.023$ GeV/c^2 [4], the expected SM values are $f_0 = 0.698$, $f_- = 0.301$, and $f_+ = 4.1 \times 10^{-4}$, with uncertainties of $\sim 0.01 - 0.02$ for f_0 and f_-, and $O(10^{-3})$ for f_+ [5]. A measurement that deviates significantly from these expectations would provide strong evidence of physics beyond the SM, indicating either a departure from the expected $V-A$ structure of the tWb vertex or the presence of a non-SM component in the $t\bar{t}$ candidate sample. We report the combination of recent measurements of f_0 and f_+ from data recorded at the Tevatron $p\bar{p}$ collider by the CDF and D0 collaborations. The measurements are combined accounting for statistical and systematic correlations using the method of Refs. [6, 7].

II. INPUT MEASUREMENTS

The inputs to the combination are the f_0 and f_+ values extracted from 2.7 fb^{-1} of CDF data in the lepton + jets ($t\bar{t} \to W^+W^-b\bar{b} \to \ell\nu q\bar{q}'b\bar{b}$) channel [8] and 5.1 fb^{-1} of CDF data in the dilepton ($t\bar{t} \to W^+W^-b\bar{b} \to \ell\nu_\ell\ell'\nu_{\ell'}b\bar{b}$) [9] channel (where ℓ and ℓ' represent an electron or a muon), and from 5.4 fb^{-1} of D0 data for lepton + jets and dilepton events together [10]. All of these measurements use data collected during Run II of the Tevatron. Assuming the unitary condition $f_- + f_0 + f_+ = 1$, two types of measurements are performed: (1) a model-independent approach where f_0 and f_+ are determined simultaneously, and (2) a model-dependent approach where f_0 (f_+) is fixed to its SM value, and f_+ (f_0) is measured. The model-independent and model-dependent approaches are referred to as "2D" and "1D," respectively. We label the input measurements as follows:

- CDF's measurements of f_0 and f_+ in the lepton + jets channel are labeled as CLf_0n and CLf_+n, respectively.
- CDF's measurements of f_0 and f_+ in the dilepton channel are labeled as CDf_0n and CDf_+n, respectively.
- D0's measurements of f_0 and f_+, which use both the lepton + jets and dilepton channels, are labeled as DBf_0n and DBf_+n, respectively.

Here $n = 1$ for 1D measurements and $n = 2$ for 2D measurements.

The CL$f_{0(+)}n$ measurements use the "matrix element" method described in Ref. [11], where the distributions of the momenta of measured jets and leptons are compared to the expectations for leading-order signal and background matrix elements, convoluted with the detector response to jets and leptons. The $t\bar{t}$ matrix elements are computed as a function of the W boson helicity fractions, so that the values of f_0 and f_+ that are most consistent with the data can be determined.

The CD$f_{0(+)}n$ and DB$f_{0(+)}n$ measurements are based on the distribution of the helicity angle $\theta^\star$ for each top quark decay, where $\theta^\star$ is the angle between the opposite of the direction of the top quark and the direction of the down-type fermion (charged lepton or d, s quark) decay product of the W boson in the W boson rest frame. The distribution ω of $\cos\theta^\star$ can be written in terms of the helicity fractions as

$$\begin{aligned}\omega(\cos\theta^\star) \;\propto\; & 2(1-\cos^2\theta^\star)f_0 + (1-\cos\theta^\star)^2 f_- \\ & +(1+\cos\theta^\star)^2 f_+.\end{aligned} \tag{1}$$

The momenta of the neutrinos, required for determining $\theta^\star$, are reconstructed in the lepton + jets channel through a constrained kinematic fit of each event, while for the dilepton channels $\theta^\star$ is obtained through an algebraic solution of the kinematics. The distribution of $\cos\theta^\star$ is then compared to the expectations from background and $t\bar{t}$ Monte Carlo (MC) simulated events, with different admixtures of helicity fractions, to determine f_0 and f_+.

CDF and D0 treat the top quark mass dependence of the measured helicity fractions differently. CDF assumes a value of $m_t = 175$ GeV when reporting central values and includes a description of how the values change as a function of m_t. D0 assumes a value of $m_t = 172.5$ GeV and assigns a systematic uncertainty to cover the m_t dependence of the result. This uncertainty corresponds to a 1.4 GeV uncertainty on m_t, accounting for both the difference between D0's assumed m_t and the world average value and the uncertainty on the world average value [3]. To facilitate the combination of results, the CDF helicity fractions are shifted to m_t of 172.5 GeV, and an uncertainty is assigned to account for the 1.4 GeV uncertainty in m_t. The input measurements are summarized in Table I.

TABLE I: Summary of the W boson helicity measurements that are used in the combinations. The CDF measurements have been shifted from their published values to reflect a change in the assumed top quark mass from 175 to 172.5 GeV. The first uncertainty in brackets is statistical and the second systematic.

CDF lepton + jets, 2.7 fb^{-1} [8]	
CL$f_0$2	$f_0 = 0.903 \pm 0.123$ [$\pm$ 0.106 $\pm$ 0.063]
CLf_+2	$f_+ = -0.195 \pm 0.090$ [$\pm$ 0.067 $\pm$ 0.060]
CL$f_0$1	$f_0 = 0.674 \pm 0.081$ [$\pm$ 0.069 $\pm$ 0.042]
CLf_+1	$f_+ = -0.044 \pm 0.053$ [$\pm$ 0.019 $\pm$ 0.050]
CDF dilepton, 5.1 fb^{-1} [9]	
CD$f_0$2	$f_0 = 0.722 \pm 0.190$ [$\pm$ 0.179 $\pm$ 0.065]
CDf_+2	$f_+ = -0.088 \pm 0.094$ [$\pm$ 0.088 $\pm$ 0.032]
CD$f_0$1	$f_0 = 0.572 \pm 0.109$ [$\pm$ 0.090 $\pm$ 0.062]
CDf_+1	$f_+ = -0.076 \pm 0.052$ [$\pm$ 0.042 $\pm$ 0.031]
D0, lepton + jets and dilepton, 5.4 fb^{-1} [10]	
DB$f_0$2	$f_0 = 0.669 \pm 0.102$ [$\pm$ 0.078 $\pm$ 0.065]
DBf_+2	$f_+ = 0.023 \pm 0.053$ [$\pm$ 0.041 $\pm$ 0.034]
DB$f_0$1	$f_0 = 0.708 \pm 0.065$ [$\pm$ 0.044 $\pm$ 0.048]
DBf_+1	$f_+ = 0.010 \pm 0.037$ [$\pm$ 0.022 $\pm$ 0.030]

III. CATEGORIES OF UNCERTAINTY

The uncertainties in the individual measurements are grouped into categories so that the correlations can be treated properly in the combination. The categories used are:

- **STA** is the statistical uncertainty. In each input 2D measurement, there is a strong anticorrelation between the values of f_0 and f_+, and values of the correlation coefficients are determined from the simultaneous fit for f_0 and f_+.
- **JES** is the uncertainty on the jet energy scale. This uncertainty can arise from theoretical uncertainties on the properties of jets, such as the model for gluon radiation, and from uncertainties in the calorimeter response. We assume that the theoretical uncertainties that are common to CDF and D0 dominate, so this uncertainty is taken to be fully correlated between CDF and D0. Details of the jet energy calibration in CDF can be found in Ref. [12].
- **SIG** is the uncertainty on the modeling of $t\bar{t}$ production and decay and has several components. The effect of uncertainties on the parton distribution functions (PDFs) are estimated using the 2×20 uncertainty sets provided for the CTEQ6M [13] PDFs. The uncertainty on the modeling of initial- and final-state gluon radiation is assessed by varying the MC parameters controlling these processes. Uncertainties from modeling hadron showers are estimated by comparing the expectations from PYTHIA and HERWIG. In addition to the above, D0 also measures the potential impact of next-to-leading order (NLO) effects by comparing the leading-order generators (ALPGEN [14], PYTHIA [15], and HERWIG [16]) with the NLO generator MC@NLO [17], uncertainties in b-quark jet fragmentation by comparing the default model [18] to an alternative version [19], and the potential uncertainty from color reconnection by comparing PYTHIA models with color reconnection turned on and off. Signal modeling uncertainties impact the CDF and D0 results in the same manner and are therefore takes as fully correlated among input measurements.
- **BGD** is the uncertainty in the modeling of background. The procedures used to estimate this uncertainty differ for the separate analyses. In CDF's dilepton measurement, the contribution of each background source is varied within its uncertainty and the resulting effect on the $\cos\theta^\star$ distribution is used to gauge the effect on the measured helicity fractions. In the CDF lepton + jets analysis, the change in the result when the background is assumed to come from only one source (e.g. only $W + b\bar{b}$ production or only multijet production), rather than from the expected mixture of sources, is taken as the uncertainty due to the background shape. The uncertainty in the background yield is evaluated by varying the signal-to-background ratio assumed in the measurement. In the D0 measurement, the $\cos\theta^\star$ distributions in data and in the background model are compared in a background-dominated sideband region. The background model in the signal region is then reweighted to reflect any differences observed in the background-dominated region, and the resulting change in the measured helicity fractions is taken as the systematic uncertainty. The correlations among the background model uncertainties in the input measurements are unknown, but presumably large because of the substantial

TABLE II: Relationship between the individual systematic uncertainties reported in Refs. [8–10] and the categories of uncertainty used for the combination.

Uncertainty category	Individual measurement uncertainties		
	CDF lepton + jets	CDF dilepton	D0 lepton + jets and dilepton
JES	Jet energy scale	Jet energy scale	Jet energy scale
			b fragmentation
SIG	ISR or FSR	Generators	$t\bar{t}$ model
	PDF	ISR or FSR	PDF
	Parton shower	PDF	
BGD	Background	Background shape	Background model
			Heavy flavor fraction
MTD	Method-related	Template statistics	Template statistics
			Analysis consistency
MTOP	Top quark mass	Top quark mass	Top quark mass
DET			Jet energy resolution
			Jet identification
			Muon identification
			Muon trigger
MHI		Instant. luminosity	

TABLE III: Values of the uncertainties from each measurement that are used in the combinations.

Measurement	STA	JES	SIG	BGD	MTD	MTOP	DET	MHI
CL$f_0$2	0.106	0.004	0.038	0.042	0.024	0.011	0.000	0.000
DB$f_0$2	0.078	0.011	0.039	0.032	0.022	0.009	0.031	0.000
CD$f_0$2	0.179	0.007	0.053	0.019	0.029	0.005	0.000	0.014
CLf_+2	0.067	0.012	0.031	0.039	0.024	0.019	0.000	0.000
DBf_+2	0.041	0.009	0.024	0.013	0.012	0.012	0.007	0.000
CDf_+2	0.088	0.014	0.023	0.005	0.015	0.005	0.000	0.001
CL$f_0$1	0.069	0.018	0.033	0.009	0.010	0.012	0.000	0.000
DB$f_0$1	0.044	0.016	0.036	0.013	0.021	0.012	0.018	0.000
CD$f_0$1	0.090	0.033	0.045	0.011	0.014	0.013	0.000	0.016
CLf_+1	0.019	0.017	0.024	0.038	0.005	0.015	0.000	0.000
DBf_+1	0.022	0.012	0.021	0.008	0.008	0.010	0.010	0.000
CDf_+1	0.042	0.019	0.021	0.004	0.007	0.007	0.000	0.008

contribution of W/Z + jets events to the background in each measurement. We therefore treat this uncertainty as fully correlated between CDF and D0, and also between measurements using dilepton and lepton + jets events.

- **MTD** are uncertainties that are specific to a given analysis method. Effects such as the limitations from the statistics of the MC and any offsets observed in self-consistency tests of the analysis are included in this category. Uncertainties in this category are fully anticorrelated for measurements of f_0 and f_+ within the same analysis, but uncorrelated between analyses.
- **MTOP** is the uncertainty due to m_t and is fully correlated between CDF and D0, and between CDF measurements.
- **DET** are uncertainties due to the response of the CDF and D0 detectors. The effects considered include uncertainty in the jet energy resolution, lepton identification efficiency, and trigger efficiency. These uncertainties are found to be negligible in the CDF measurements, but are larger in the D0 measurements due to discrepancies observed in muon distributions between data control samples and MC. While the cause of these discrepancies was subsequently understood and resolved, D0 assigns a systematic uncertainty to cover the effect rather than re-analyzing the data.
- **MHI** is the uncertainty due to multiple hadronic interactions in a single bunch crossing. This uncertainty pertains only to the CDF dilepton measurement, since in D0's measurements the distribution of instantaneous luminosities in the MC events is reweighted to match that in the data sample, thereby accounting for the impact of multiple interactions, and in CDF's lepton + jets measurement this uncertainty is found to be negligible.

The relationships between the individual uncertainties reported in Refs. [8–10] and the above categories are given in Table II, and the values of the uncertainties from each input measurement are given in Table III.

TABLE IV: The statistical correlation coefficients among the measurements used in the combination.

	CLf_0	DBf_0	CDf_0	CLf_+	DBf_+	CDf_+
CLf_0	1.0	0.0	0.0	−0.6	0.0	0.0
DBf_0	0.0	1.0	0.0	0.0	−0.8	0.0
CDf_0	0.0	0.0	1.0	0.0	0.0	−0.9
CLf_+	−0.6	0.0	0.0	1.0	0.0	0.0
DBf_+	0.0	−0.8	0.0	0.0	1.0	0.0
CDf_+	0.0	0.0	−0.9	0.0	0.0	1.0

TABLE V: The correlation coefficients among the measurements used in the combination for the JES, SIG, BGD, and MTOP systematic uncertainties.

	CLf_0	DBf_0	CDf_0	CLf_+	DBf_+	CDf_+
CLf_0	1.0	1.0	1.0	−1.0	−1.0	−1.0
DBf_0	1.0	1.0	1.0	−1.0	−1.0	−1.0
CDf_0	1.0	1.0	1.0	−1.0	−1.0	−1.0
CLf_+	−1.0	−1.0	−1.0	1.0	1.0	1.0
DBf_+	−1.0	−1.0	−1.0	1.0	1.0	1.0
CDf_+	−1.0	−1.0	−1.0	1.0	1.0	1.0

IV. COMBINATION PROCEDURE

The results are combined using the procedure described in Ref. [6] to define the best linear unbiased estimators of the correlated observables f_0 and f_+. The method uses all the measurements and their covariance matrix $\mathbf{M}$, where $\mathbf{M}$ is the sum of the covariance matrices for each category of uncertainty (for the 1D measurements, only the sub-matrices corresponding to the helicity fraction that is varied are relevant):

$$\begin{aligned}\mathbf{M} \;=\; & \mathbf{M}_{\rm STA} + \mathbf{M}_{\rm JES} + \mathbf{M}_{\rm SIG} + \mathbf{M}_{\rm BGD} \\ & + \mathbf{M}_{\rm MTD} + \mathbf{M}_{\rm MTOP} + \mathbf{M}_{\rm DET} + \mathbf{M}_{\rm MHI}.\end{aligned} \tag{2}$$

The correlation coefficients assumed when populating the covariance matrices, for each category of uncertainty, are given in Tables IV–VII. When correlations in systematic uncertainties exist between measurements of f_0 and f_+, the correlation coefficients are taken to be -1, reflecting the large negative statistical correlations observed between measurements of f_0 and f_+ within a given analysis.

V. RESULTS

The result of the combination of the 2D measurements is

$$\begin{aligned} f_0 &= 0.732 \pm 0.081 \\ &\quad [\pm\, 0.063\ (\text{stat.}) \pm 0.052\ (\text{syst.})], \\ f_+ &= -0.039 \pm 0.045 \\ &\quad [\pm\, 0.034\ (\text{stat.}) \pm 0.030\ (\text{syst.})]. \end{aligned} \tag{3}$$

TABLE VI: The correlation coefficients among the measurements used in the combination for the MTD systematic uncertainty.

	CLf_0	DBf_0	CDf_0	CLf_+	DBf_+	CDf_+
CLf_0	1.0	0.0	0.0	−1.0	0.0	0.0
DBf_0	0.0	1.0	0.0	0.0	−1.0	0.0
CDf_0	0.0	0.0	1.0	0.0	0.0	−1.0
CLf_+	−1.0	0.0	0.0	1.0	0.0	0.0
DBf_+	0.0	−1.0	0.0	0.0	1.0	0.0
CDf_+	0.0	0.0	−1.0	0.0	0.0	1.0

TABLE VII: The correlation coefficients among the measurements used in the combination for the DET and MHI systematic uncertainties.

	CLf_0	DBf_0	CDf_0	CLf_+	DBf_+	CDf_+
CLf_0	1.0	0.0	1.0	−1.0	0.0	−1.0
DBf_0	0.0	1.0	0.0	0.0	−1.0	0.0
CDf_0	1.0	0.0	1.0	−1.0	0.0	−1.0
CLf_+	−1.0	0.0	−1.0	1.0	0.0	1.0
DBf_+	0.0	−1.0	0.0	0.0	1.0	0.0
CDf_+	−1.0	0.0	−1.0	1.0	0.0	1.0

TABLE VIII: The contribution from each category of systematic uncertainty in the combined measurements.

Category	2D combination		1D combination	
	δf_0	δf_+	δf_0	δf_+
JES	0.008	0.010	0.016	0.018
SIG	0.037	0.022	0.021	0.036
BGD	0.027	0.012	0.009	0.012
MTD	0.014	0.008	0.006	0.007
MTOP	0.016	0.010	0.010	0.012
DET	0.016	0.003	0.007	0.011
MHI	0.001	0.012	0.002	0.002

The contribution of each category of systematic uncertainty is shown in Table VIII. The combination has a χ^2 value of 6.67 for four degrees of freedom, corresponding to a p-value of 7% for consistency of the input measurements. The combined values of f_0 and f_+ have a correlation coefficient of -0.86. The consistency of each input measurement with the combined value and the weight that each input measurement contributes to the combined result is given in Table IX. In some cases, the weights have negative values, which can occur in the presence of correlated uncertainties when the most likely value of the observable lies outside of the range of the input measurements [7] or, in the case of simultaneous measurements of correlated quantities, when negative weights are needed to satisfy the normalization condition that the weights sum to unity [6]. Contours of constant χ^2 in the f_0 and f_+ plane are shown in Fig. 1. The SM values for the helicity fractions lie within the 68% C.L. contour of probability.

Combination of the 1D measurements yields:

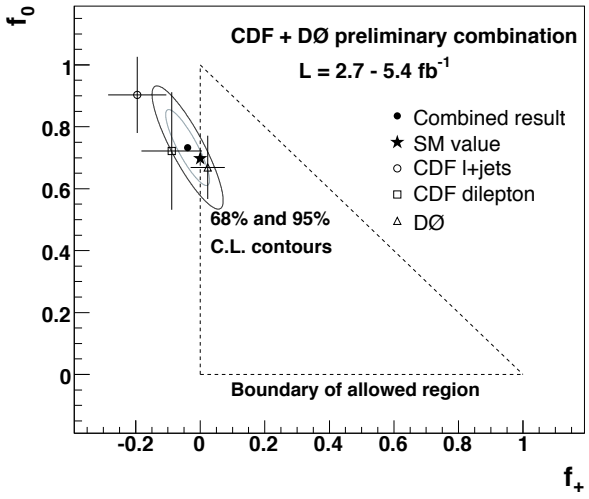

FIG. 1: Contours of constant χ^2 for the combination of the 2D helicity measurements. The ellipses indicate the 68% and 95% C.L. contours, the dot shows the best-fit value, the triangle corresponds to the physically allowed region where f_0 and f_+ are non-negative and sum to ≤ 1, and the star marks the expectation from the SM. The measurements input to the combination are represented by the open circle, square, and triangle, with error bars indicating the 1σ uncertainties on f_0 and f_+.

TABLE IX: The number of standard deviations of each 2D measurement from the combined values of f_0 and f_+, and the relative weight contributed by each to the combination.

Measurement	s.d. from combined values	Weight for f_0 (%)	Weight for f_+ (%)
CL$f_0$2	1.85	45.2	−15.6
DB$f_0$2	−1.04	49.6	4.7
CD$f_0$2	−0.06	5.2	10.9
CLf_+2	−2.00	28.9	−3.8
DBf_+2	2.17	−13.2	67.8
CDf_+2	−0.59	−15.8	36.0

TABLE X: The number of standard deviations of each 1D measurement from the combined values of f_0 and f_+, and the relative weight contributed by each to the combination.

Measurement	s.d. from combined values	Weight (%)
CL$f_0$1	0.19	31.5
DB$f_0$1	0.75	59.3
CD$f_0$1	−1.21	9.2
CLf_+1	−0.76	5.5
DBf_+1	1.81	71.6
CDf_+1	−1.63	22.9

$$\begin{aligned} f_0 &= 0.685 \pm 0.057 \\ &\quad [\pm\ 0.035\ (\text{stat.}) \pm 0.045\ (\text{syst.})], \\ f_+ &= -0.013 \pm 0.035 \\ &\quad [\pm\ 0.018\ (\text{stat.}) \pm 0.030\ (\text{syst.})]. \end{aligned} \tag{4}$$

The contribution of each category of systematic uncertainty is shown in Table VIII. The combination for f_0 (f_+) has a χ^2 of 1.64 (3.53) for two degrees of freedom, corresponding to a p-value of 44% (17%) for consistency among the input measurements. The consistency of each input measurement with the combined value and the weight that each input measurement contributes to the combined result are presented in Table X.

VI. SUMMARY

We have combined measurements of the helicity of W bosons arising from top quark decay in $t\bar{t}$ events from the CDF and D0 collaborations, finding

$$\begin{aligned} f_0 &= 0.732 \pm 0.081 \\ &\quad [\pm\ 0.063\ (\text{stat.}) \pm 0.052\ (\text{syst.})], \\ f_+ &= -0.039 \pm 0.045 \\ &\quad [\pm\ 0.034\ (\text{stat.}) \pm 0.030\ (\text{syst.})] \end{aligned} \tag{5}$$

for measurements in which both f_0 and f_+ are varied simultaneously, and

$$\begin{aligned} f_0 &= 0.685 \pm 0.057 \\ &\quad [\pm\ 0.035\ (\text{stat.}) \pm 0.045\ (\text{syst.})], \\ f_+ &= -0.013 \pm 0.035 \\ &\quad [\pm\ 0.018\ (\text{stat.}) \pm 0.031\ (\text{syst.})]. \end{aligned} \tag{6}$$

when one of the helicity fractions is held fixed at the SM value.

These are the most precise measurements of f_0 and f_+ to date. The results are consistent with expectations from the SM and provide no indication of new physics in the tWb coupling nor of the presence of a non-SM source of events in the selected sample.

VII. ACKNOWLEDGEMENT

We thank the staffs at Fermilab and collaborating institutions, and acknowledge support from the DOE and NSF (USA); CEA and CNRS/IN2P3 (France); FASI, Rosatom and RFBR (Russia); CNPq, FAPERJ, FAPESP and FUNDUNESP (Brazil); DAE and DST (India); INFN (Italy); Ministry of Education, Culture, Sports, Science and Technology (Japan); Colciencias (Colombia); CONACyT (Mexico); World Class University Program, National Research Foundation, KRF and KOSEF (Korea); CONICET and UBACyT (Argentina); Australian Research Council (Australia); FOM (The Netherlands); STFC and the Royal Society (United Kingdom); MSMT and GACR (Czech Republic); CRC Program and NSERC (Canada); Academy of Finland (Finland); BMBF and DFG (Germany); SFI (Ireland); Slovak R&D Agency (Slovakia); Programa Consolider-Ingenio 2010 (Spain); The Swedish Research Council (Sweden); Swiss National Science Foundation (Switzerland); NSC (Republic of China); CAS and CNSF (China) and the A.P. Sloan Foundation (USA).

---

[1] F. Abe *et al.* (CDF Collaboration), Phys. Rev. Lett. **74**, 2626 (1995).
[2] S. Abachi *et al.* (D0 Collaboration), Phys. Rev. Lett. **74**, 2632 (1995).
[3] Tevatron Electroweak Working Group, arXiv:1007.3178[hep-ex] (2010).
[4] K. Nakamura *et al.* (Particle Data Group), J. Phys. G **37**, 075021 (2010).
[5] M. Fischer *et al.*, Phys. Rev. D **63**, 031501(R) (2001).
[6] A. Valassi, Nucl. Instrum. Methods in Phys. Res. A **500**, 391 (2003).
[7] L. Lyons and D. Gibaut, Nucl. Instrum. Methods in Phys. Res. A **270**, 110 (1998).
[8] T. Aaltonen *et al.*, (CDF Collaboration), Phys. Rev. Lett. **105**, 042002 (2010).
[9]
[10] V.M. Abazov *et al.* (D0 Collaboration), Phys. Rev. D **83**, 032009 (2011).
[11] V.M. Abazov *et al.* (D0 Collaboration), Nature **429**, 638 (2004).
[12] A. Bhattia *et al.*, Nucl. Instrum. Methods in Phys. Res. A **566**, 375 (2006).
[13] J. Pumplin *et al.*, J. High Energy Phys. **07**, 012 (2002).
[14] M.L. Mangano, J. High Energy Phys. **07**, 001 (2003).
[15] T. Sjöstrand *et al.*, Computer Phys. Commun. **135** 238, (2001).
[16] G. Corcella *et al.*, J. High Energy Phys. **01**, 010 (2001).
[17] S. Frixione and B. Webber, J. High Energy Phys. **06**, 29 (2002).
[18] M.G. Bowler, Z. Phys. C **11** 169 (1981).
[19] Y. Peters *et al.*, FERMILAB-TM-2425-E (2006).